ISOPE 2009 — *The 19th International Offshore and Polar Engineering Conference*
Osaka, Japan, June 21–26, 2009

Nonlinear Multi-Mode Interactions in Subsea Risers Undergoing Vortex-Induced Vibrations

Narakorn Srinil [a,b], *Marian Wiercigroch* [a], *Patrick O'Brien* [b]

[a]Centre for Applied Dynamics Research, School of Engineering, University of Aberdeen, King's College, Scotland, UK

[b]MCS, Aberdeen, Scotland, UK

ABSTRACT

This paper investigates nonlinear multi-mode interactions in subsea risers undergoing vortex-induced vibrations based on a computationally efficient reduced-order fluid-structure interaction model. Cross-flow responses as a result of a steady uniform current are considered. The geometrically nonlinear equations of riser motion are coupled with nonlinear wake oscillators which have been modified to capture the effect of initial curvatures of curved cylinder and to approximate the space-time varying hydrodynamic lift forces. The main objectives are to provide new insights into the vortex-induced vibration characteristics of risers under external and internal resonances and to distinguish nonlinear dynamic behaviors between curved catenary and straight top-tensioned risers. The analyses of multi-mode contributions, lock-in regimes, response amplitudes, resonant nonlinear modes and curvatures are carried out and several interesting aspects are highlighted.

KEY WORDS: Subsea riser; vortex-induced vibration; wake oscillator; fluid-structure interaction; reduced-order model; multi-mode interaction; resonant nonlinear mode.

INTRODUCTION

Nonlinear multi-mode interactions due to resonance excitations in mechanical continuous structures have been the subject of considerable research in the last 30 years (Nayfeh 2000). This is due to the fact that resonant multi-mode interactions are responsible for large-amplitude vibrations which potentially give rise to premature fatigue failures of structural systems. In subsea applications, a resonance mechanism of a cylindrical flexible structure subject to vortex-induced vibration (VIV) occurs when the vortex-shedding frequency locks on to one (or more) of the structural natural frequencies. This external resonance takes place in a certain range of the reduced flow velocity known as lock-in or synchronization region. Moreover, if system natural frequencies are closely spaced and commensurable in a nearly integer ratio, the vibrating structure may further experience a so-called internal resonance. The combination of external and internal resonances signifies a worst dynamic scenario which is often unavoidable for a long slender structure having a large number of degrees of freedom and natural frequencies.

In this study, a robust reduced-order fluid-solid interaction model and numerical integration scheme, developed by the authors (Srinil *et al*., 2008), is considered in an attempt to investigate the multi-mode dynamic interactions of subsea risers undergoing VIV. As cross-flow responses are typically greater than in-line responses (Sarpkaya 2004), attention is focused on the analysis of cross-flow VIV, along with the qualitative and quantitative comparison in nonlinear dynamics between a steel catenary riser (SCR) and a straight top-tensioned riser (TTR). The geometrically nonlinear equations of riser motion are based on a tensioned beam or flexural cable model with pinned-pinned boundary conditions. The empirical hydrodynamic model is based on a distributed wake oscillator approximating the space-time varying lift forces. Because the multi-mode coupling effect is expected to be relatively pronounced, both structural and fluid nonlinearities are fully accounted for. To the authors' knowledge, a very few studies in literature deal with the application of wake-structure interaction models to the *multi-mode* VIV problems, particularly for slender *curved* risers (SCRs). Moreover, there is a lack of comparison in the ensuing nonlinear dynamics between SCR and TTR. For this reason, we aim to fill this gap by implementing the multi-mode wake-riser interaction model for the VIV investigation of both curved and straight risers.

From a modeling viewpoint of vortex shedding, a wake oscillator is scrutinized as simplified, phenomenological and semi-empirical model that provides a researcher an understanding of some fundamental nonlinear phenomena of VIV, in spite of the fact that there is no involvement in the flow characterization (Gabbai and Benaroya 2005). Some *ad hoc* assumptions are common in analytical models. These comprise, e.g., the consideration of nominal two-dimensional flow at all times, the full correlation length of vortex shedding along the cylinder length (i.e., under lock-in condition) and the neglected effects of end boundaries and stream-wise cylinder movement. To produce a benchmarking series of empirical wake coefficients vs. physical parameters, rigid and elastically-mounted cylinders in a uniform flow have been mostly considered in different experimental campaigns. Nevertheless, wake-oscillator models have enjoyed some success in the numerical-experimental comparison of VIV response predictions of straight risers (Facchinetti *et al*. 2004, Violette *et al*. 2007). Moreover, the computations based on wake-body interaction models are generally fast with respect to direct numerical simulations. These are very helpful towards industrial applications, where sea current flows are actually at high Reynolds number (Re) regimes (Sumer and Fredsoe 1999).

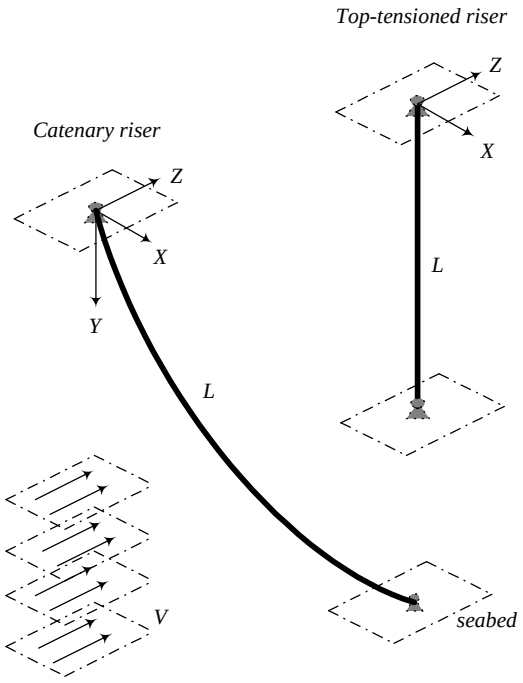

Fig. 1 Models of SCR and TTR subject to uniform current flow

WAKE-RISER MULTI-MODE INTERACTION MODEL

Following Srinil *et al*. (2008, 2009), a continuum model of arbitrarily sagged inclined SCR and straight vertical TTR, displayed in Fig. 1, is considered. With reference to the global Cartesian coordinate system, the riser with equilibrium length L is connected from a stationary floating structure to seabed with pinned-pinned supports. A horizontal offset X_H and water depth Y_H define a chord inclination angle of SCR ($\theta_r = \tan^{-1} Y_H/X_H$). A steady incoming flow is in the Z^+-direction, which is perpendicular to the equilibrium plane (XY) of initial curvatures in the case of SCR. As our attention is focused on the prediction of cross-flow VIV, both horizontal (transversal) and vertical (axial) dynamic displacements from a reference static catenary (straight) configuration are evaluated for SCR (TTR). For convenience in the analytical modeling which relies on continuous functions, it is assumed that a planar static configuration of SCR is solely due to its effective self weight and is described by an exact closed-form hyperbolic-function formula. The bending restraint and current flow action are considered to play a role after the settlement of static equilibrium. The nonlinear partial-differential equations of riser motion about static configuration are expressed in a general dimensional form as

$$(m+m_a)\frac{\partial^2 u}{\partial t^2}+c\frac{\partial u}{\partial t} = \frac{\partial}{\partial s}\left\{T\left(\frac{\partial u}{\partial s}\right)+EA_r\left(\frac{\partial x}{\partial s}\frac{\partial u}{\partial s}+\frac{\partial y}{\partial s}\frac{\partial v}{\partial s}+\frac{1}{2}\left(\left(\frac{\partial u}{\partial s}\right)^2+\left(\frac{\partial v}{\partial s}\right)^2\right)\right)\left(\frac{\partial x}{\partial s}+\frac{\partial u}{\partial s}\right)-EI\frac{\partial}{\partial s}\left(\frac{\partial^2 u}{\partial s^2}\right)\right\}+H_1, \quad (1)$$

$$(m+m_a)\frac{\partial^2 v}{\partial t^2}+c\frac{\partial v}{\partial t} = \frac{\partial}{\partial s}\left\{T\left(\frac{\partial v}{\partial s}\right)+EA_r\left(\frac{\partial x}{\partial s}\frac{\partial u}{\partial s}+\frac{\partial y}{\partial s}\frac{\partial v}{\partial s}+\frac{1}{2}\left(\left(\frac{\partial u}{\partial s}\right)^2+\left(\frac{\partial v}{\partial s}\right)^2\right)\right)\left(\frac{\partial y}{\partial s}+\frac{\partial v}{\partial s}\right)-EI\frac{\partial}{\partial s}\left(\frac{\partial^2 v}{\partial s^2}\right)\right\}+H_2, \quad (2)$$

by considering the riser as a flexural elastic beam-cable (or tensioned-beam) satisfying the Euler-Bernoulli hypothesis. s denotes Lagrangian coordinate, u (x) and v (y) represent dynamic (static) displacement in horizontal or transversal (X) and vertical or axial (Y) direction in the case of SCR or TTR, respectively. For TTRs, $x = y = 0$. Riser properties are considered to be uniform, with hydrodynamic diameter (D), mass (m), potential added mass ($m_a = C_A\rho A_r$, with A_r being the effective cross-sectional area, ρ the fluid density and C_A=1), structural damping (c), bending (EI) and axial (EA_r) stiffness. T denotes axial static tension which is considered to be non-uniform (uniform) for SCR (TTR) and H_i denotes hydrodynamic forces leading to cross-flow VIV. The effects of shear, torsion, seabed and internal flow-induced friction forces, which are quite important for SCRs, are not herein considered. Nevertheless, the effect of geometrical nonlinearities, meaningful for multi-mode coupling and interactions (Srinil *et al*. 2007), is accounted for. Because current flow is normal to SCR plane, the cross-flow VIV due to normal lift force F_L corresponds to SCR in-plane motion. By neglecting the tangential hydrodynamics, the unsteady excitation lift forces per unit length read (Skop and Balasubramanian 1997, Srinil *et al*. 2008, 2009)

$$H_1 = -F_L\sin\theta = \frac{1}{2}\rho DV^2\left(Q_x - 2\gamma\dot{u}/\omega_s\right), \quad (3)$$

$$H_2 = F_L\cos\theta = \frac{1}{2}\rho DV^2\left(Q_y - 2\gamma\dot{v}/\omega_s\right), \quad (4)$$

where V is the current flow velocity, γ is a stall parameter, Q_x and Q_y are the corresponding wake parameters described by the following van der Pol nonlinear oscillators (Srinil *et al*. 2008, 2009)

$$\frac{\ddot{Q}_X}{\sin\theta}-\frac{\omega_S G C_{L0}^2\dot{Q}_X}{\sin\theta}+\frac{4\omega_S G Q_X^2\dot{Q}_X}{\sin^3\theta}+\frac{\omega_S^2 Q_X}{\sin\theta}=\frac{\omega_S F\dot{u}}{\sin\theta}, \quad (5)$$

$$\frac{\ddot{Q}_Y}{\cos\theta}-\frac{\omega_S G C_{L0}^2\dot{Q}_Y}{\cos\theta}+\frac{4\omega_S G Q_Y^2\dot{Q}_Y}{\cos^3\theta}+\frac{\omega_S^2 Q_Y}{\cos\theta}=\frac{\omega_S F\dot{v}}{\cos\theta}, \quad (6)$$

in which C_{L0} is the lift coefficient of a stationary cylinder, a dot denotes differentiation with respect to time t. The vortex-shedding frequency (rad/s) in the wake (ω_S) is unique such that $\omega_S = 2\pi\mathrm{St}V/D$, where St is the Strouhal number. The space-dependent local angle θ is measured clockwise from the horizontal X-axis and can be analytically obtained from the SCR static equilibrium analysis. F and G are empirical coefficients obtained by calibrating with a series of experimental results which generally include the measurement of maximum response amplitudes of (rigid/flexible) cylinders and the vortex-to-structural frequency ratio during VIV (Skop and Balasubramanian 1997). They depend on the mass-damping (so-called Skop-Griffin) parameter $S_G = \xi/\mu$, where ξ is the modal damping and μ is the mass ratio given by

$$\mu = \frac{\rho D^2}{8\pi^2\mathrm{St}^2\left(m+m_a\right)}. \quad (7)$$

It is worth emphasizing that the nonlinear wake oscillators Eqs. (5-6) are dependent on *both* time and space variables. One may also account for the Re effect through wake coefficients (Srinil *et al*. 2009). Q_X and Q_Y are to be determined together with u and v. For TTRs, only Eq. (5) is considered with $\sin\theta$=1. In the following, the horizontal displacement coordinate x (in lieu of s) is alternatively used as the independent space parameter. Moreover, the differential Eqs.(1-2) and (5-6) are rearranged in their temporal first-order forms. For convenience in the parametric studies, overall displacement variables in the associated equations are normalized with respect to D.

By considering both geometric and hydrodynamic nonlinearities, it is assumed that a two-way coupled riser-wake response contains spatial contributions from some excited modes whose natural frequencies are in the neighborhood of the vortex-shedding frequency. Based on the modal expansion approach, both displacement (u, v) and associated velocity (defined as A_i, B_i) variables of riser and wake in Eqs. (1-2) and (5-6) are postulated in terms of N riser modes as

$$\begin{aligned} \dot{u} = A_1 \rightarrow \quad & u = \sum_{n=1}^{N} f_n \phi_n, \quad A_1 = \sum_{n=1}^{N} p_n \phi_n, \\ \dot{v} = A_2 \rightarrow \quad & v = \sum_{n=1}^{N} f_n \varphi_n, \quad A_2 = \sum_{n=1}^{N} p_n \varphi_n. \end{aligned} \tag{8}$$

$$\begin{aligned} \dot{Q}_x = B_1 \rightarrow \quad & Q_x = \sum_{n=1}^{N} d_n \phi_n, \quad B_1 = \sum_{n=1}^{N} e_n \phi_n, \\ \dot{Q}_y = B_2 \rightarrow \quad & Q_y = \sum_{n=1}^{N} d_n \varphi_n, \quad B_2 = \sum_{n=1}^{N} e_n \varphi_n. \end{aligned} \tag{9}$$

where ϕ_n and φ_n are horizontal and vertical displacement components of n^{th} mode shape functions associated with natural frequencies (in water) ω_n of the riser. They are obtained based on a Fourier sine series in conjunction with a hybrid analytical-numerical solution of linear equations governing free undamped motion in Eqs. (1-2) with bending and extensibility effects (Srinil *et al*. 2008). In Eqs. (8-9), f_n (d_n), p_n (e_n) denote generalized coordinates of riser (wake) to be determined. By substituting Eqs. (8-9) into (1-2) and (5-6), performing the standard Galerkin procedure with zero displacements and curvatures at end boundaries, and applying the orthonormalization of modes, a system of nonlinear ordinary-differential equations describing the wake-riser interactions are expressed as (Srinil *et al*. 2009)

$$\begin{aligned} & \dot{f}_n = p_n, \\ & \dot{p}_n = -2\xi_n \omega_n p_n - \omega_n^2 f_n + \mu \omega_n^2 (d_n - \frac{2\gamma}{\omega_s} p_n) + \sum_{i=1}^{N}\sum_{j=1}^{N} \Lambda_{nij} f_i f_j \\ & \quad + \sum_{i=1}^{N}\sum_{j=1}^{N}\sum_{k=1}^{N} \Gamma_{nijk} f_i f_j f_k, \\ & \dot{d}_n = e_n, \\ & \dot{e}_n = \omega_s G C_{L0}^2 e_n - \omega_s^2 d_n + \omega_s F p_n + \\ & \quad \sum_{\substack{i=1, \\ i \neq n}}^{N} \Pi_{ni} \left(\omega_s G C_{L0}^2 e_i - \omega_s^2 d_i + \omega_s F p_i \right) - 4\omega_s G \sum_{i=1}^{N}\sum_{j=1}^{N}\sum_{k=1}^{N} \Re_{nijk} d_i d_j e_k, \end{aligned} \tag{10-13}$$

where quadratic/cubic nonlinear coefficients accounting for multi-mode contributions and interactions read

$$\begin{aligned} \Lambda_{nij} &= -c_r \int_0^{X_H/D} \frac{1}{k^3} \left(\frac{3}{2}\phi_n'\phi_i'\phi_j' + y'\phi_n'\phi_i'\varphi_j' + \frac{1}{2}\phi_n'\varphi_i'\varphi_j' + \varphi_n'\phi_i'\varphi_j' + \right. \\ & \qquad \left. \frac{y'}{2}\varphi_n'\phi_i'\phi_j' + \frac{3}{2}y'\varphi_n'\varphi_i'\varphi_j' \right) dx, \\ \Gamma_{nijk} &= -\frac{c_r}{2} \int_0^{X_H/D} \frac{1}{k^3} \left(\phi_n'\phi_i'\phi_j'\phi_k' + \phi_n'\phi_i'\varphi_j'\varphi_k' + \varphi_n'\phi_i'\phi_j'\varphi_k' + \varphi_n'\varphi_i'\varphi_j'\varphi_k' \right) dx, \\ \Pi_{ni} &= \int_0^{X_H/D} k \left(\frac{\phi_n\phi_i}{y'} + \varphi_n\varphi_i \right) dx \Big/ \int_0^{X_H/D} k \left(\frac{\phi_n^2}{y'} + \varphi_n^2 \right) dx, \\ \Re_{nijk} &= \int_0^{X_H/D} k^3 \left(\frac{\phi_n\phi_i\phi_j\phi_k}{y'^3} + \varphi_n\varphi_i\varphi_j\varphi_k \right) dx \Big/ \int_0^{X_H/D} k \left(\frac{\phi_n^2}{y'} + \varphi_n^2 \right) dx. \end{aligned} \tag{14-17}$$

Note that a dash denotes differentiation with respect to x, $k = (1+y'^2)^{1/2}$, $c_r = EA_r/(m+m_a)D^2$. Eqs. (14-17) are numerically integrated based on a 64-point Gaussian Quadrature. Parameters k and y' vanish in the case of TTR. Depending on the number of considered riser N modes, the total N^2 (N^3) quadratic (cubic) coefficients in each n equation are calculated *a priori*. Eq.(13) entails N coupled van der Pol oscillators with identical vortex frequency ω_s. In turn, they are coupled with nonlinear structural oscillators through associated p-terms. The overall $4N$ equations (10-13) are simultaneously and systematically solved in time domain by a numerical integration method with a stable time stepping and proper initial conditions of displacement and velocity. The riser VIV response depends on the mass-damping parameter, static configuration profile (in the case of SCR), modal shape functions (e.g., Fig. 2), tuning of system vortex and natural frequencies, strength of fluid-structure nonlinearities, empirical wake coefficients (F, G). In addition, the riser dynamic behavior depends on whether the cable (tension) or the beam (bending) effect predominates. This may be characterized by a single dimensionless *tensioned-beam* parameter $\Delta = L(T_a/EI)^{1/2}$, where T_a is the SCR tension at maximum sag or the TTR uniform (averaged) tension (Srinil *et al*. 2008, 2009). The cable-predominant SCR has a greater value of Δ ($\approx O(10^{-3})$). As regards empirical wake coefficients, through lack of actual experimental data associated with each n^{th} mode, F and G are considered to be the same, or mode-independent, in all wake oscillators for a given set of system parameters. The important effect of Re on the F and G variation and thus the VIV response predictions is herein disregarded. This aspect has recently been discussed in Srinil *et al*. (2009) with relevant analyses and results.

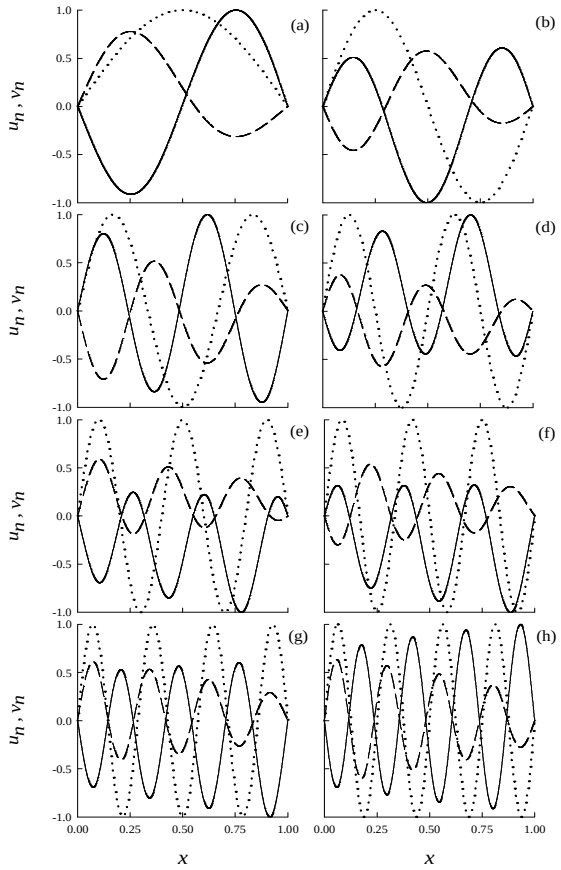

Fig. 2 Normalized displacement shapes for first 8 in-plane modes (a-h) of risers with $\Delta = 272$: dashed and solid (dotted) lines denote u_n and v_n of SCR (u_n of corresponding TTR), respectively.

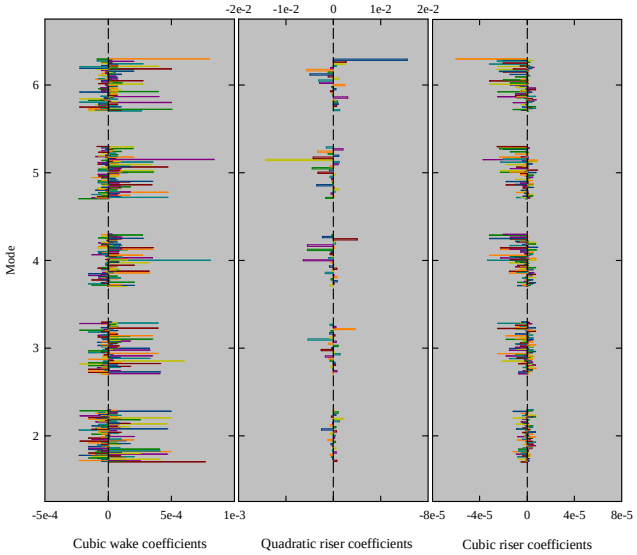

Fig. 3 Variation of nonlinear coefficients with mode number for SCR

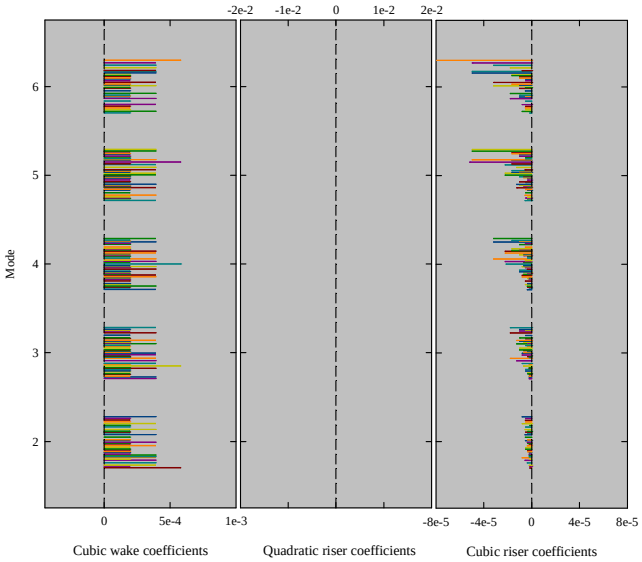

Fig. 4 Variation of nonlinear coefficients with mode number for TTR

NUMERICAL RESULTS AND DISCUSSION

Our aim is to numerically investigate the multi-mode VIV responses of SCR in comparison with those of TTR through a reduced-order fluid-riser interaction model having a minimum DOF. For given system parameters and a range of flow velocities, a convergence study with varying N modes should be made when integrating Eqs. (10)-(13). As exemplified by Srinil *et al.* (2009), both qualitative and quantitative errors take place when considering a single-mode $N = 1$ (or very-low DOF) solution for VIV of SCR. Hence, the multi-mode analysis is essential. In the following, nonlinear interaction coefficients in Eqs. (14)-(17) are first analyzed prior to evaluating the VIV responses.

Nonlinear Multi-Mode Interaction Coefficients

As an example, the tension-dominated SCR with $\Delta = 272$ whose data are given in Srinil *et al.* (2009) is considered. The corresponding normalized modal shape functions (u_n, v_n) for the first 8 in-plane modes are displayed in Fig. 2, along with those (only u_n as axial displacement v_n is very small and negligible) of the TTR having $\Delta = 272$. Based on the assumed sine-based series, Fig. 2 distinguishes the modal shapes as well as relative phase characteristics between SCR and TTR, the former exhibiting the asymmetrical (i.e. neither symmetric nor anti-symmetric) shapes due to the inclination and varying initial curvature effects (Srinil and Rega 2007) whereas the latter exhibiting the typical string mode shapes. This qualitative distinction subsequently affects the associated nonlinear interaction coefficients as shown in Figs. 3 and 4 with $N = 5$ (n = 2-6) for SCR and TTR, respectively. The cubic wake (Eq. 17) and riser (Eq. 15) coefficients for each n^{th} mode of SCR reflect both positive and negative non-trivial values with high fluctuation (Fig. 3), whereas those of TTR reflect either positive (Eq. 17) or negative (Eq. 15) values with much lower fluctuation (Fig. 4). Several zero cubic coefficients are also found for TTR. Indeed, in the absence of k and y' in Eq. (17) of TTR, the cubic wake coefficients entail a series of coefficients with the same magnitudes for different n because of the same orthogonality properties of symmetric vs. anti-symmetric modes being applied. On the contrary, the corresponding quadratic riser coefficients (Eq. 14) are completely trivial again owing to the effective nonlinear orthogonalities (Srinil and Rega 2007). This is in contrast to Fig. 3 where quadratic coefficients are non-trivial for SCR. Overall, both quadratic and cubic riser coefficients increase with increasing mode number. The high fluctuation (+/-) of coefficient values of SCR (Fig. 3) has a major influence both on the nonlinear damping terms in wake oscillators and on the strength of geometric (softening/hardening) nonlinearities, depending on the response amplitudes. Throughout Figs. 2-4, these meaningful comparative aspects of nonlinear interaction coefficients between SCR and TTR allow us to signal the differences in the ensuing VIV responses which will be discussed in the following.

Multi-Mode Interactions in Catenary and Top-Tensioned Risers

As riser cross-flow VIV responses in the global coordinate system (Fig. 1) consist of horizontal u and vertical v displacements, the resulting maximum amplitude of each modal coordinate (A_n/D) is calculated by

$$A_n / D = \mathrm{Max}\sqrt{\left(f_n\phi_n\right)^2 + \left(f_n\varphi_n\right)^2}, \tag{18}$$

in which maximum ϕ_n and φ_n, and f_n are independently determined from the eigenfunction and transient-free time histories analysis, respectively. The *effective* maximum response amplitude of riser – accounting for overall modal contributions and actual relative phases in both time series and shape functions (Fig. 2) – can be determined through Eq. (8), depending on the number of modes N accounted for.

By considering the SCR (Figs. 2-4) with $N = 5$ (n = 2-6) and $N = 7$ (n = 1-7) and assuming that S_G ($\xi = 0.01$) parameters are identical for all modes, the VIV amplitude response diagrams in the case of increasing V are comparatively highlighted in Fig.5. These plots are useful in evaluating (i) the potential multi-mode lock-in, (ii) the maximum amplitudes, (iii) the solution convergence with varying N, (iv) the sharing, switching and interaction of modes when varying the system control parameter (i.e. V). As shown in Fig. 5, the hysteresis effect with solution jumps is typical for a self-limiting character. It is worth emphasizing that the overlapping of modal amplitudes takes place in a particular range of V and the sharing strength may be low or high depending on the tuning of corresponding natural frequencies. It is seen that the 5th and 6th modes are the most strongly-coupled since their frequencies (2.168 and 2.228 rad/sec) are nearly 1:1 internally-resonant apart from being resonant with the varying wake frequencies (as per varying V). Such modal sharing and interactions can be also seen through time histories (Srinil *et al.* 2009). These highlight the occurrence of multi-mode lock-in or synchronization whereby the wake

and riser frequencies are externally and internally resonant. When comparing the responses with N=5 (symbols) and N=7 (line series), overall responses are seen to coincide in a large V range. However, the lower (n = 1) and higher (n = 7) modes share the dynamic solution with N = 7 when V < 0.35 and V > 0.88 m/s, respectively. Up to 4 modes (n = 4-7) could interact in a marginal V range (0.88 < V < 0.93 m/s), with the 4th mode solution exhibiting a secondary small-amplitude peak. Thus, to account for such multi-mode interactions, the 5-mode solution would be sufficient and valid in the approximate range between 0.35 < V < 0.88 m/s. This valid range would become even narrower if further decreasing N. The amplitude A_n/D responses in Fig. 5 may be also described by a variation of the reduced flow velocity parameter U_r=2$\pi V/\omega_n D$, where ω_n is the natural frequency in water of each relevant mode. As shown in Fig. 6, the dependency of VIV on a normalized parameter U_r is indeed helpful in comparing the extent of lock-in bandwidth of each individual mode and characterizing which mode is more or less crucial. Overall, the maximum A_n/D are in between 1 < A_n/D < 2 and the synchronization occurs in the typical primary range of 4 < U_r < 8. These are in good agreement with well-known cross-flow VIV characteristics of rigid and flexible cylinders (see, e.g., Fujarra *et al*. 2001, Willden and Graham 2006).

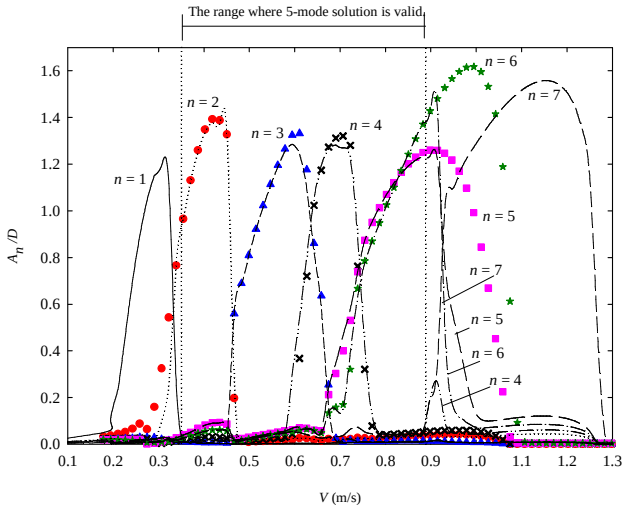

Fig. 5 VIV amplitude response diagrams *vs*. V for SCR with N = 5 (n = 2-6, symbol series) and N = 7 (n = 1-7, line series)

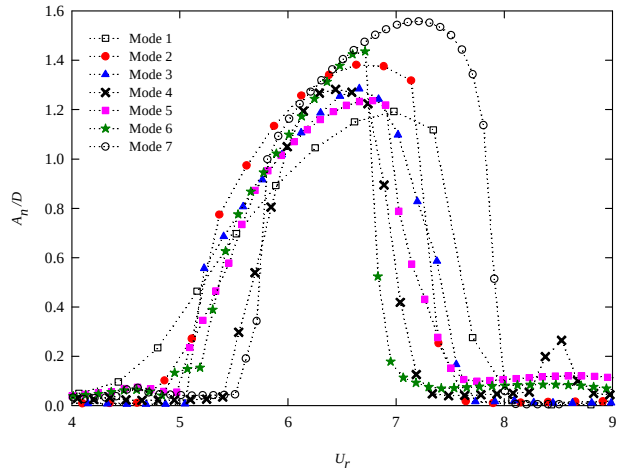

Fig. 6 VIV amplitude response diagrams *vs*. U_r for SCR with N = 7

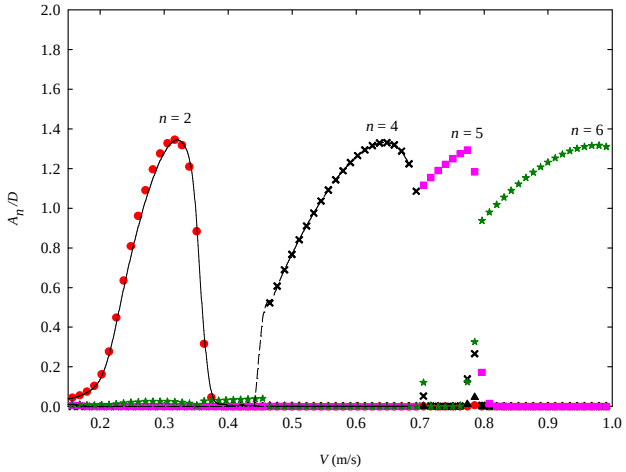

Fig. 7 VIV amplitude response diagrams *vs*. V for TTR with N = 5 (n = 2-6, symbol series) and N = 3 (n = 2-4, line series)

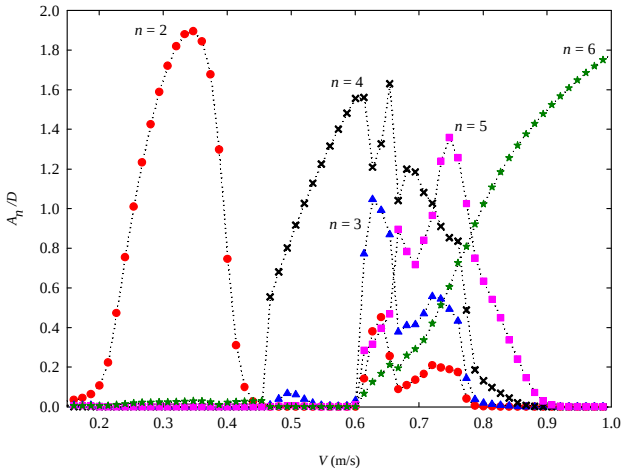

Fig. 8 VIV amplitude response diagrams *vs*. V for TTR with N = 5 (n = 2-6): decreased damping by order of magnitude with respect to Fig. 7

When considering TTR with the same Δ and S_G (damping) as in the case of SCR (Fig. 5), both quantitative and qualitative differences take place in the amplitude response diagrams, as highlighted in Fig. 7 with N = 5 (n = 2-6). It can be seen that the 3rd-mode solution disappears, leading to a small gap (0.38 < V < 0.45 m/s) in which the VIV response is completely trivial. This occurs even though the 3-mode solution with n = 2-4 is considered (solid and dashed lines in Fig. 7). In addition, there is no appreciable overlapping or sharing of modes: only mode switching is seen and each modal response stays in its own lock-in regime as V is increased. Unlike Fig. 5, overall maximum amplitudes are nearly comparable ($A_n/D \approx 1.4$). This may be attributed to the fact that nonlinear cubic wake coefficients of each mode are quantitatively and qualitatively analogous (Fig. 4). Nevertheless, the overall VIV responses dramatically change when decreasing the modal damping (as well as S_G) by an order of magnitude (ξ = 0.003) with respect to that (ξ = 0.01) being considered in Fig.7. As highlighted in Fig. 8, a relatively strong modal interaction occurs in a large V range. Overall amplitudes increase and somewhat fluctuate. In particular, the 3rd-mode response (which vanishes in Fig. 7) comes into play and strongly interacts with the higher 4th, 5th and 6th mode responses, along with the lower 2nd mode which is resonantly driven into the response once again after its role in the primary lock-in regime. Two (n = 3, 5) or three (n = 4) major

peaks are possible. In addition, the resemblance to the so-called "initial" and "lower" branches in amplitude response diagrams of elastically-mounted rigid (Khalak and Williamson 1997) and flexible (Fujarra *et al*. 2001) cylinders is noticed for n = 2, 3.

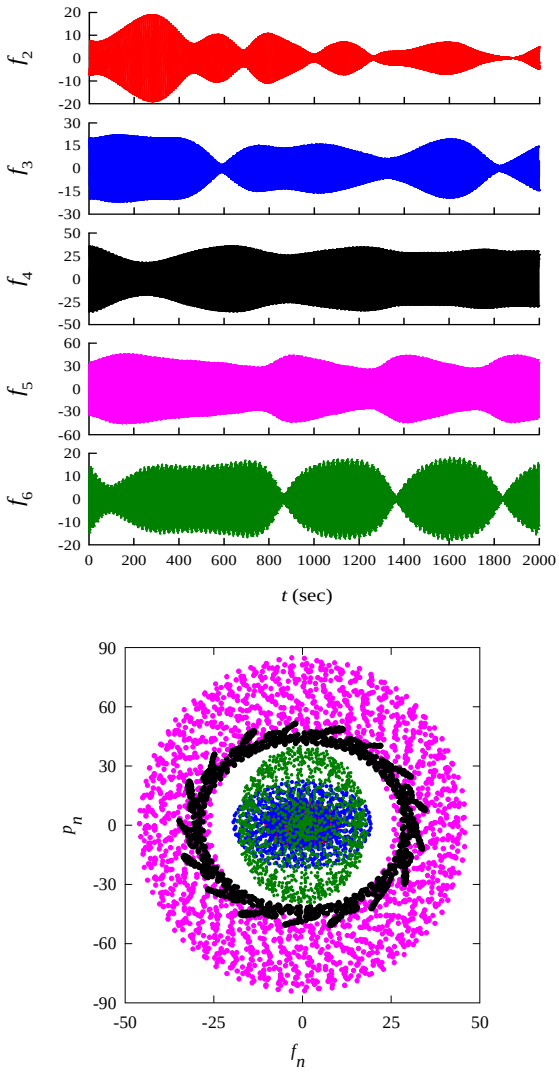

Fig. 9 Nonlinear time histories and corresponding phase portraits of each riser modal coordinate in Fig.8 with V = 0.734 m/s

With reference to Fig. 8, it is also interesting to examine nonlinear time histories of riser displacement coordinates (f_n) and the associated phase portraits (i.e., f_n vs. p_n) to gain better understanding into the temporal behavior of multi-mode sharing and interactions. As visualized in Fig. 9 with V = 0.734 m/s, a beating-like phenomenon – which is a typical modal interaction feature due to external or internal resonance – is remarkable in all time histories. The transient dynamics are rich depending on initial conditions, and the VIV amplitudes are highly modulated throughout the recorded timeframe (2000 sec.). The phase plots also reveal circle-like orbits which guarantee the periodicity or "limit cycle" of overall modal responses, albeit with high modulations (inner and outer rings). As depicted in Fig. 8, the 5th mode is seen to play the most predominant role in the modal interactions for the given flow velocity and system parameters. Indeed, from Fig. 8, $A_2/D \approx 0.20$, $A_3/D \approx 0.54$, $A_4/D \approx 0.91$, $A_5/D \approx 1.24$ and $A_6/D \approx 0.51$.

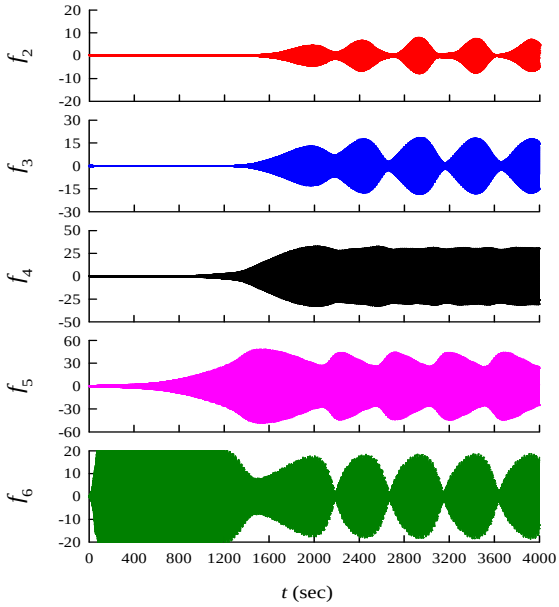

Fig. 10 Nonlinear time histories with nearly "at-rest" initial conditions

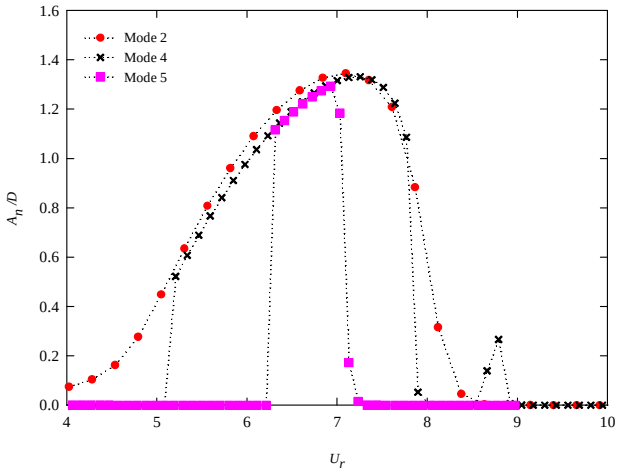

Fig. 11 VIV amplitude response diagrams *vs*. U_r for TTR in Fig.7

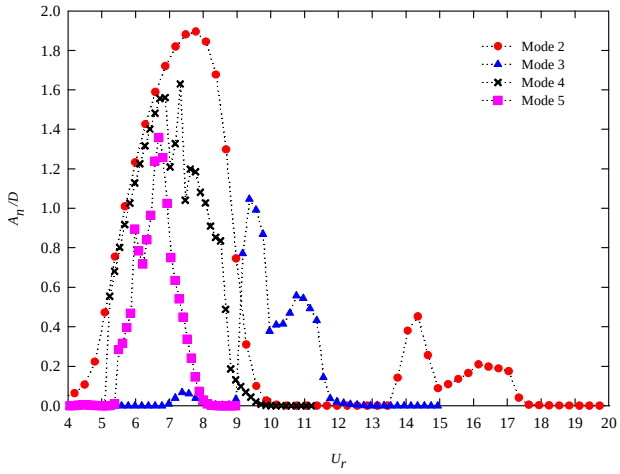

Fig. 12 VIV amplitude response diagrams *vs*. U_r for TTR in Fig.8

The effect of initial conditions on VIV prediction is now highlighted. Corresponding to Fig. 8 with V = 0.734 m/s and n = 2-6, the condition of nearly "at rest", where riser is slightly disturbed from its static equilibrium, is assigned in numerical integrations and the time responses are plotted in Fig. 10 in comparison with Fig. 9 which is based on higher-amplitude initiations. It can be seen that, initially, the 6th mode response grows rapidly and becomes steady. It totally predominates the VIV up to t = 1200 sec. This is the expected circumstance as the relevant natural frequency (0.349 Hz) is the most nearly close to the vortex frequency (0.382 Hz). However, as the time moves on (t >1200 sec), other lower modes are resonantly excited, sharing and strongly interacting with each other. The beating frequencies change with higher amplitude modulations, with respect to Fig. 9. The 4th mode response seems to be the most stable and steady. When overall modal interactions become stabilized, maximum modal amplitudes in both Figs. 9 and 10 are comparable, with the 5th mode being the dominating one. Such switching in the dominating mode during the VIV and the associated time sharing concept have recently been discussed based on experimental testing and frequency domain results of flexible risers (Swithenbank 2007, Lie *et al*. 2008).

The extent of each lock-in bandwidth in Figs. 7 and 8 is now discussed through Figs. 11 and 12, respectively. In comparison with Fig. 6 (SCR) that shows nearly-comparable lock-in ranges ($4 < U_r < 8$) of different modes, Fig. 11 (TTR) reveals both wider (n = 2) and narrower (n = 5) lock-in regions depending on the excited mode. Thus, the strength of wake-riser interactions of SCR is seen to be greater than TTR when given the same system parameters. When decreasing ξ for TTR, both primary (n = 2, 4, 5) and secondary (n = 2, 3) lock-in regions take place in Fig. 12 with U_r being extended to 20. The occurrence of secondary lock-in at higher U_r, accompanied by smaller response amplitudes, has been recently discussed by Willden and Graham (2006) based on CFD simulations of an elastically-mounted rigid cylinder at low Re = 50-400. They have considered a cylinder with low mass ratios (m^* = 5 and 10, where $m^* = 4m/\pi\rho D^2$) and zero damping, and defined this regime as "super-harmonically" excited response. This super-harmonic character is observed in Fig. 12 with $m^* \approx 8$ and very low damping ξ = 0.003. Because of assuming St = 0.2, the primary lock-in is centered near $U_r \approx 5$ ($\omega_s/\omega_n = 1$) for n = 2, 4, 5, whereas the secondary lock-in is centered near $U_r \approx 10$ ($\omega_s/\omega_n = 2$) for n = 3 and near $U_r \approx 15$ ($\omega_s/\omega_n = 3$) for n = 2, respectively. The main difference is that, herein, the flexible cylinder is considered and the flow is in a sub-critical range (Sumer and Fredsoe 1999) with much higher Re ($4x10^4 < Re < 3x10^5$).

Resonant Nonlinear Modes/Curvatures of Riser Undergoing VIV

It has been highlighted that nonlinear multi-mode interactions in both SCR and TTR undergoing VIV occur in a certain lock-in or U_r range, depending on overall fluid-structure parameters (mass-damping, vortex vs. natural frequencies, strength of nonlinearities, wake coefficients). Based on the obtained amplitudes, the ensuing displacement profiles or "resonant nonlinear modes" of risers – which are very important in subsequent analyses of curvatures, stresses and fatigue damage – can be evaluated *a posteriori* through Eq.(8). With reference to Figs. 1, 2, 5 and 6 (with N=5), the normalized nonlinear planar modes in horizontal u_n and vertical v_n directions of SCR are illustrated in Fig. 13 with four chosen V. For each U_r, resonant nonlinear modes at different 5 time snapshots – each of which occurs when one of the corresponding modal coordinates f_n (n = 2-6, respectively) attends its maximum state in the time history during multi-mode interactions – are visualized with monochrome lines. Actual relative phases amongst the modes at each time instant are thus accounted for. The resulting spatial multi-mode superimposition depends on the linear continuous shape functions (Fig. 2) obtained from the eigenvalue analysis.

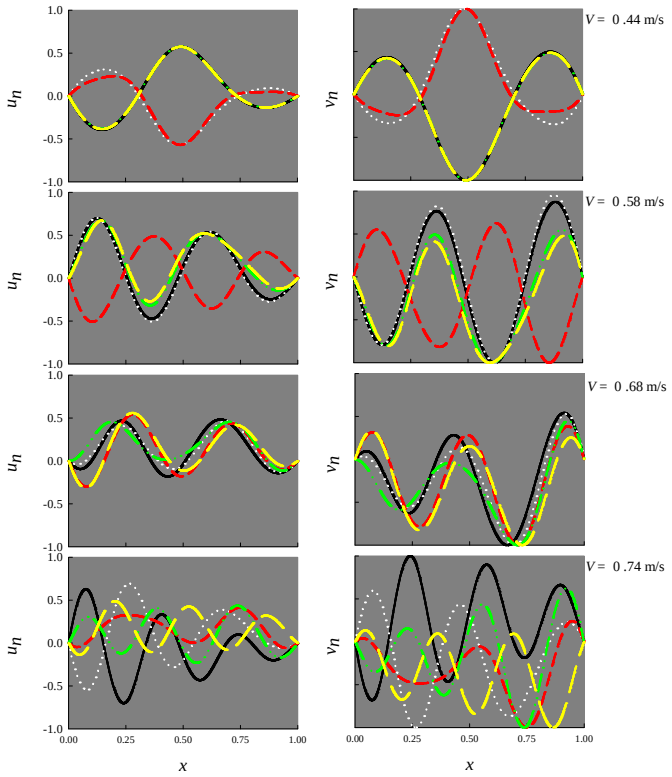

Fig. 13 Nonlinear modes of SCR undergoing VIV at 5 time instants

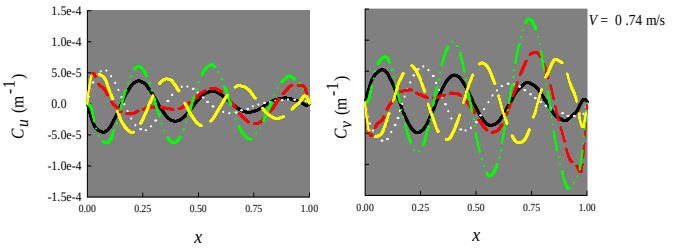

Fig. 14 Nonlinear curvatures of SCR undergoing VIV at 5 time instants

As shown in Fig. 13, the space-time modifications of nonlinear mode shapes are quite remarkable. When the VIV response is dominated by a single (e.g., 2nd or 3rd) mode (V = 0.44 or 0.58 m/s), the positions – where maximum (anti-node) and minimum (node) amplitudes occur – do not significantly change with time. Thus, linear and nonlinear modes appear analogous. Nevertheless, when the multi-mode (n = 3, 4 or n = 4, 5, 6) VIV response occurs (V = 0.68 or 0.74 m/s), a resemblance to a single mode shape is not amenable. The node/anti-node amplitudes (as well as relevant phases) spatially and temporally vary, depending on modal contributions, amplitudes and the level of space-time sharing, observed through the amplitude response diagrams and time histories. Overall, resonant nonlinear single and multi modes are asymmetrical with respect to middle span owing to the underlying effect of SCR inclination and varying initial curvatures. For TTRs, the resonant nonlinear modes may be asymmetric if multi symmetric/anti-symmetric modes are involved in the VIV responses. Based on Fig. 13, the associated profiles of nonlinear curvatures (C_u, C_v) can be also evaluated, as shown in Fig. 14 (V=0.74 m/s). In essence, the space-time distributions of displacements and curvatures allow us to determine their maximum values which will be very useful in the inspection of riser stress and fatigue damage.

CONCLUSIONS

Multi-mode cross-flow VIV responses of curved SCR and straight TTR have been investigated based on a robust reduced-order wake-riser interaction model. The effects of geometrical nonlinearities and varying initial curvatures of SCR static configuration are fully taken into account through the equations of riser motion and the nonlinear wake oscillators approximating the distributed (space-time) hydrodynamics. Depending on the number of potentially vortex-excited modes, analyses of multi modal contributions have been performed through nonlinear interaction coefficients. Owing to the effect of initial curvatures and the inherent feature of system asymmetry of SCR, the ensuing results highlight qualitatively different coefficients between SCR and TTR.

The amplitude response diagrams have been constructed in the case of increasing flow velocity. To attain solution convergence, the number of considered modes has been varied. Depending on overall fluid-structure properties, e.g., the mass-damping parameter, the commensurability of vortex and riser natural frequencies, the strength of nonlinearities and empirical coefficients, the predicted VIV responses based on a time-domain approach reveal the important features of multi-mode lock-in regimes, multi-mode sharing, switching and interactions, as well as qualitative and quantitative differences in nonlinear dynamics between SCR and TTR. The occurrence of external and internal resonances notably influences modal interactions. In addition, the assigned initial conditions play a significant role in the transient dynamics, the time sharing and the onset of limit cycles of associated time histories. When considering a very low structural damping, the existence of super-harmonic responses in a secondary lock-in regime, associated with higher reduced velocities, has been noticed. This characteristic is in good qualitative agreement with recent CFD studies of rigid-cylinder free vibrations. Finally, resonant nonlinear modes of riser undergoing VIV and their space-time modifications have been evaluated. In contrast to single-mode VIV, the multi-mode VIV reveals meaningful spatial sharing of modes, with varying amplitudes and relative phases along riser. As a result of multi-mode interactions and system asymmetry (SCR), nonlinear and linear modes are qualitatively distinctive. These are practically useful for riser design since relevant maximum curvatures, stresses and fatigue damage are of importance.

The effects of Re and structural geometric nonlinearities on the multi-mode VIV predictions have been highlighted by Srinil *et al*. (2009). Overall analysis results demonstrate how the developed reduced-order wake-riser interaction model may be very helpful in explaining some intriguing phenomena recently observed by experimental testing, apart from robustly predicting the multi-mode VIV of deepwater SCRs and TTRs. These are achieved within minutes of the computation which are far quicker than those performed by the CFD-based simulations. Nonetheless, the wake oscillators and associated empirical coefficients need further calibration, revision and verification so that they will actually capture multi-mode interactions between cross-flow/in-line VIV due to either uniform or sheared flows. These can be realized by a new series of CFD or experimental results which are being rigorously considered worldwide. (e.g., Dahl *et al*. 2006, Miliou *et al*. 2007).

ACKNOWLEDGEMENTS

The authors gratefully acknowledge the support from the Knowledge Transfer Partnerships (KTP).

REFERENCES

Dahl, JM, Hover, FS, Triantafyllou, MS (2006). "Two-degree-of-freedom vortex-induced vibrations using a force assisted apparatus," *J Fluids Str*, Vol 22, pp 807-818.

Facchinetti, M, de Langre, E, Biolley, F (2004). "Coupling of structure and wake oscillators in vortex-induced vibrations," *J Fluids Str*, Vol 19, pp 123-140.

Fujarra, AL, Pesce, CP, Flemming, F, Williamson, CHK (2001). "Vortex-induced vibration of a flexible cantilever," *J Fluids Str*, Vol 15, 651-658.

Gabbai, RD, Benaroya, H, (2005). "An overview of modeling and experiments of vortex-induced vibration of circular cylinders," *J Sound Vib*, Vol 82, 575-616.

Khalak, A, Williamson, CHK (1997). "Investigation of the relative effects of mass and damping in vortex-induced vibration of a circular cylinder," *J Wind Eng Industrial Aerodyn*, Vol 69-71, pp 341-350.

Lie, H, Larsen, CM, Kaasen, KE (2008). "Frequency domain model for prediction of stochastic vortex induced vibrations for deepwater risers," *Proc. The 27th OMAE*, Paper No.57566, pp 1-13.

Miliou, A, De Vecchi, A, Sherwin, SJ, Graham, JMR (2007). "Wake dynamics of external flow past a curved circular cylinder with the free stream aligned with the plane of curvature," *J Fluids Mech*, Vol 592, pp 89-115.

Nayfeh, AH (2000) *Nonlinear Interactions: Analytical, Computational and Experimental Methods*, Wiley, New York

Sarpkaya, T (2004). "A critical review of the intrinsic nature of vortex-induced vibrations," *J Fluids Str*, Vol 19, pp 389-447.

Skop, RA, Balasubramanian, S (1997). "A new twist on an old model for vortex-excited vibrations," *J Fluids Str*, Vol 11, pp 395-412.

Srinil, N, Rega, G, Chucheepsakul, S (2007). "Two-to-one resonant multi-modal dynamics of horizontal/inclined cables. Part I: Theoretical formulation and model validation," *Nonlinear Dyn*, Vol 48, pp 231-252.

Srinil, N, Rega, G (2007). "Two-to-one resonant multi-modal dynamics of horizontal/inclined cables. Part II: Internal resonance activation, reduced-order models and nonlinear normal modes," *Nonlinear Dyn*, Vol 48, pp 253-274.

Srinil, N, Wiercigroch, M, O'Brien, P, Lane, M (2008), "New model for vortex-induced vibration of catenary riser", *Proc. The 8th ISOPE Pacific/Asia Offshore Mech Sym*, Bangkok, pp129-136.

Srinil, N, Wiercigroch, M, O'Brien, P, Younger, R (2009), "Vortex-induced vibration of catenary riser: reduced-order modeling and lock-in analysis using wake oscillator", in *Proc. The 28th OMAE*, Paper No.79166, pp.1-11.

Sumer, BM, Fredsoe, J (1997). *Hydrodynamics around Cylindrical Structures*, World Scientific, Singapore.

Swithenbank, SB (2007). "Dynamics of long flexible cylinders at high-mode number in uniform and sheared flows," PhD Thesis, MIT

Violette, R, de Langre, E, Szydlowski, J (2007). "Computation of vortex-induced vibration of long structures using a wake oscillator model: comparison with DNS and experiments," *Computer Str*, Vol 85, 1134-1141.

Willden, RHJ, Graham, JMR (2006). "Three distinct response regimes for the transverse vortex-induced vibrations of circular cylinders at low Reynolds numbers," *J Fluids Str*, Vol 22, pp 885-895.